Stability of Airplanes in Ground Effect

R. W. Staufenbiel* and U.-J. Schlichting†
Technical University Aachen, Aachen, Federal Republic of Germany

In ground effect, the aerodynamic coefficients vary considerably with height. Longitudinal motion in ground effect reveals modes and stability conditions remarkably different from out-of-ground characteristics, a fact that has a large impact on a successful concept of "wing-in-ground" vehicles. Using calculated aerodynamic coefficients and a linearized approach, static and dynamic stabilities were studied for a chosen more conventional configuration. In addition, flare maneuvers were studied for an aircraft equipped with a simple two-term controller. It is shown that the performance of the controller is considerably influenced by the ground effect. The interrelation between height-dependent aerodynamic coefficients and longitudinal stability is explained and shows particular importance in flare maneuvers.

Nomenclature

A,B,C,D,E,F	= coefficients of the characteristic equation (B1)
A_R,B_R,C_R,D_R,E_R	= coefficients of the characteristic equation (B4) with flight controller included
C_D,C_L,C_m	= aerodynamic coefficients
$\bar{c}$	= mean aerodynamic chord
h	= c.g. position as a fraction of $\bar{c}$
h_n	= position of neutral point
H	= height of mean quarter-chord point above ground
HS	= measure of static height stability defined in Eq. (1)
i_y	= radius of gyration in pitch
K	= nondimensional gain of the two-term controller defined in Eq. (B5)
l_y	$= \bar{c}/i_y$
s	= Laplace variable
S	= wing area
t_n	= unit of time, $= v_n/g$
T_v	= time constant of the controller defined in Eq. (B3)
v_n	= unit of speed, $= \sqrt{(W/S)/(\rho/2)}$
$\hat{v}$	= nondimensional speed, $= V/v_n$
V_R	= gain of controller defined in Eq. (B3)
V_S	= vertical velocity at touchdown
W	= total weight of the aircraft
z	$= H/\bar{c}$
α	= angle of attack
γ	= flight path angle
μ	= relative mass parameter, $= W/\rho S g \bar{c}$
τ	= nondimensional time, $= t/t_n$
τ_v	$= T_v/t_n$

Subscripts

0	= initial state

Received June 11, 1986; revision received March 12, 1987.

*Professor of Aerospace Engineering, Department of Aerospace Engineering. Associate Fellow AIAA.

†Research Engineer, Department of Aerospace Engineering; currently with Diehl GmbH & Co., Röthenbach, FRG.

Introduction

AIRCRAFT move close to the ground during takeoff and landing. During these phases of flight, the ground distance is relatively small in comparison with the dimensions of the airplane and the ground effect is expected to influence the aerodynamic characteristics considerably. The basic nature of the changes in the aerodynamic coefficients in ground proximity has been well known for some time, the result of both experiments and theoretical models. One of the earliest contributions, published in 1921, was directed toward the performance aspect of the ground effect, which was analyzed through a simple model based on the Prandtl lifting-line theory.[1] More recently, Gratzer and Mahal[2] discussed in detail the characteristics of STOL aircraft near the ground and explored the influence of the more important aircraft design parameters, primarily the performance aspects for takeoff and landing. For investigating flight characteristics in ground proximity, perturbation terms (depending on height) have been added to the equations of motion (see, e.g., Ref. 3).

The influence of ground effect on flying qualities was of particular interest for the concept of "wing-in-ground effect vehicles" (WIG's), which intentionally operate within ground effect for a long time. In several papers, the static and dynamic longitudinal stability of WIG's in linearized approaches were studied[4-6] and the investigation then extended into the area of nonlinear effects.[7-9] From these studies, it was concluded that the characteristics of longitudinal stability in ground effect can have considerable influence on the landing paths, particularly on the flareout from the approach path. The relationship between the longitudinal stability characteristics and the flare maneuver is illustrated in Fig. 1, in which the flare technique is considered to be an excited phugoid.[10] Better knowledge of this relationship in ground proximity may contribute to a more realistic design of simulators and flight controllers. Then, pilot control of a difficult flareout situation could be improved, and the danger of accidents during this critical phase of flight might be diminished.

In the next section, aerodynamic coefficients, calculated by a panel method, will show the general effects of ground proximity. For this principal investigation, a wing with a rectangular planform and trailing-edge flaps has been chosen. Based on the lift and pitching moment coefficient, depending on height, the "static height stability" will be introduced as an important stability measure in ground effect. Then, the dynamic longitudinal stability will be discussed without and with a flight controller optimized for automatic flare maneuver. The paper concludes with a presentation of the simulation results illustrating the ground influence on the flare maneuver,

which is evidently related to the adverse static and dynamic stability characteristics in ground proximity.

Aerodynamic Characteristics of Airfoils and Wings in Ground Effect

The flow around an airfoil or a wing is considerably modified under the influence of ground effect. A typical modification of the streamlines around an airfoil of moderate camber is shown in Fig. 2 at different heights above the ground. By diminishing the ground distance, the streamlines become increasingly rectified, and their density is reduced at the lower side of the airfoil, leading to an increase of pressure called the "ram effect." On the upper side, the streamlines show a reduction in the effective camber, which results in a distinct decrease of the suction pressure.

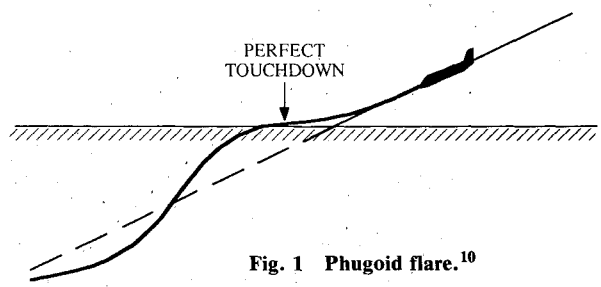

Fig. 1 Phugoid flare.[10]

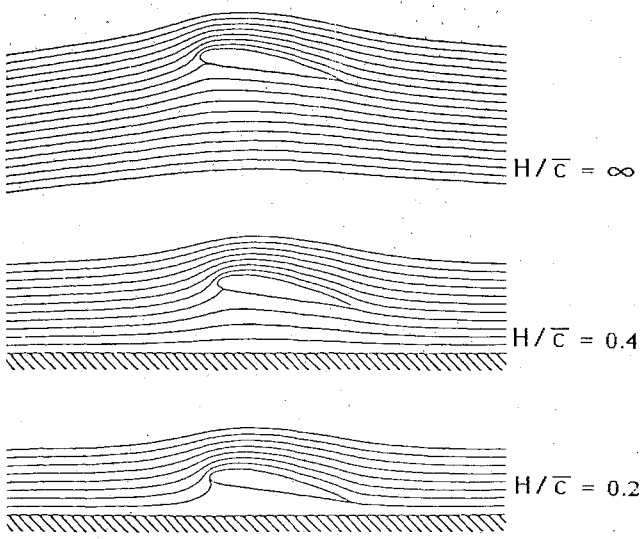

Fig. 2 Streamlines around an airfoil for various heights above ground.

The lift and pitching moment coefficients are shown in Fig. 3 as a function of angle of attack and height for a Clark-Y airfoil. For this moderate cambered airfoil, the ram effect prevails, and a gain of lift is obtained over a wide range of angles of attack. For the chosen location of the center of gravity, the static stability margin is positive. If the airfoil is trimmed for higher lift coefficients ($C_L > 0.5$), a decrease in height will result in a reduction of lift, which can be considered to be a static instability in height. Therefore, the condition of "static height stability" (HS) was introduced in Ref. 5, given by

$$\mathrm{HS} \equiv \left(\frac{\partial C_L}{\partial z}\right)_{C_m} < 0 \tag{1}$$

Using the concept of derivatives in the form

$$\delta C_L = C_{L\alpha}\delta\alpha + C_{Lz}\delta z$$

$$\delta C_m = C_{m\alpha}\delta\alpha + C_{mz}\delta z \tag{2}$$

it follows that

$$\delta C_L = \left[C_{Lz} - \left(\frac{C_{mz}}{C_{m\alpha}}\right)C_{L\alpha}\right]\delta z + \left(\frac{C_{L\alpha}}{C_{m\alpha}}\right)\delta C_m \tag{3}$$

Thus, the stability equation (1) can be written as

$$\mathrm{HS} = C_{Lz} - (C_{mz}/C_{m\alpha})C_{L\alpha} < 0 \tag{4}$$

If the influence of ground effect on pitching is neglected (equivalent to $C_{mz} = 0$), Eq. (4) reduces to

$$\mathrm{HS} = C_{Lz} < 0 \tag{5}$$

Under this constraint, the Clark-Y airfoil is stable in height ($C_{Lz} < 0$ due to Fig. 3b).

If the static stability margin is constant (independent of the angle of attack and height), the relationship

$$C_m = C_{m0} - C_L(h_N - h) \tag{6}$$

leads to

$$\mathrm{HS} = 0 \tag{7}$$

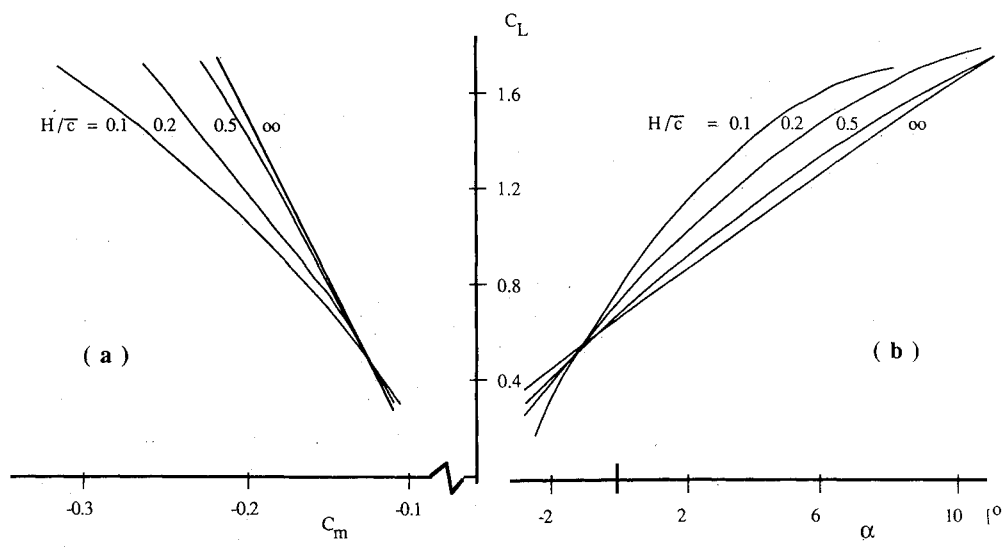

Fig. 3 Lift and pitching moment coefficients of a Clark-Y airfoil.

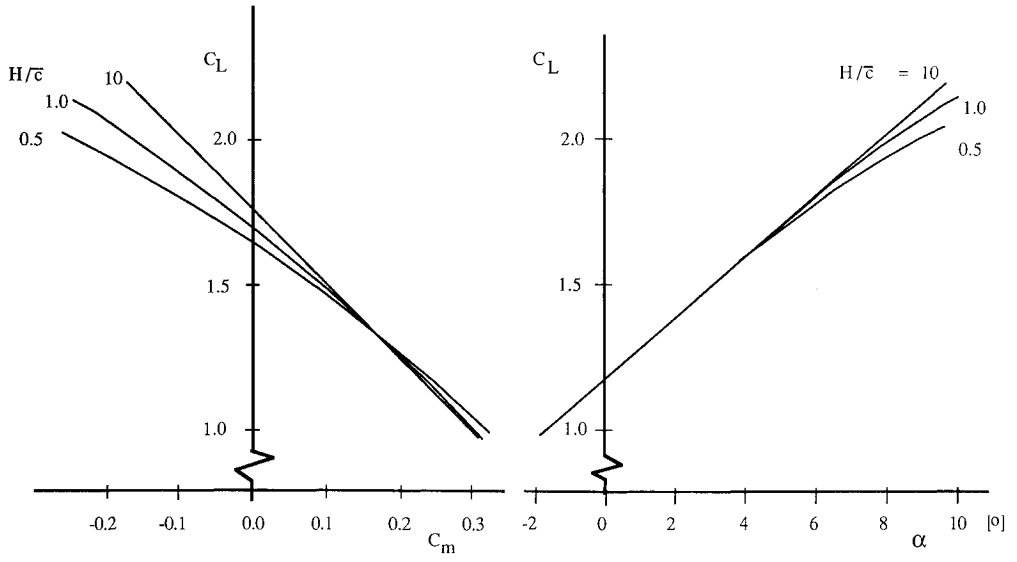

Fig. 4 Lift and pitching moment coefficients for an aircraft configuration described in Appendix B.

This means that the increase in lift at lower heights (as seen in Fig. 3b) is just offset by a reduction in the angle of attack because of a nose-down pitching moment. In this case, the airfoil is neutrally stable in height. Thus, the reason for the height instability of airfoils is the fact that, in general, the neutral point is shifted backward, mainly due to the ram effect. As shown in Refs. 6 and 7, it is possible to find special airfoils, characterized by an S-type mean line, that are stable in height over a range of lift coefficients.

Unlike the static stability in the pitching motion, height stability cannot be achieved by shifting the center of gravity. The reason can be easily understood from Fig. 3a. A change in the c.g. position will rotate the bundle of moment curves as a whole without changing the sequence of the curves, such that HS will not change the sign. But stability in height can be achieved by incorporating horizontal tails working out of the ground effect. Then, the absolute value of $C_{m\alpha}$ increases, while C_{mz} is not changed. This will reduce the value of the normally adverse second term in Eq. (4).

If a finite wing approaches the ground, a decrease in the induced angle of attack can be observed as an additional ground effect. This effect is favorable insofar as the lift increase leads to a more negative C_{Lz}. Furthermore, the horizontal tail is influenced by the ground effect. Whereas only a weak direct influence of the ground effect is expected, the indirect influence originating from a reduction in the downwash is considerable. It results in a favorable increase of tail efficiency and an adverse nose-down pitching moment.

These finite wing effects certainly depend on the aspect ratio. For configurations with a high horizontal tail and wings of small or moderate aspect ratios, height stability can be achieved. To give an example, for a typical WIG vehicle (X-113, see Refs. 6 and 11) with a low aspect ratio of 1.7, the derivatives for a height of $z = H/\bar{c} = 1$ and the chosen c.g. position are

$$C_{L\alpha} = 3.2, \qquad C_{Lz} = -0.035$$
$$C_{m\alpha} = -0.7, \qquad C_{mz} = 0.003$$

Then, the stability condition [Eq. (4)] is met, in terms of the above figures, by

$$\mathrm{HS} = -0.035 + 0.014 = -0.21 < 0 \tag{8}$$

For this vehicle, the stabilizing effect of C_{Lz} exceeds the destabilizing influence of the nose-down pitching motion, given by the second term in Eq. (8).

A completely different and unstable behavior is shown in Fig. 4. Notice that, for lift coefficients above 1.3, a disturbance in height changes the lift in such a way that the airplane is carried away from the trimmed height. These characteristics have been found in a wing/tailplane configuration having a rectangular wing of aspect ratio 10. The static stability margin chosen is 0.3. For a typical WIG vehicle, the aspects of static and dynamic longitudinal stability have been discussed in Refs. 5–8. In this paper, we are concerned with the more conventional high-aspect-ratio wing/tailplane configuration, the aerodynamic coefficients of which are shown in Fig. 4.

Longitudinal Stability and Flare Maneuvers in Ground Effect

For a more complete evaluation of flight qualities in the presence of the ground effect, it is necessary to consider the dynamic stability. The longitudinal equations of motion used for this purpose are given in Appendix A. For the purpose of stability investigations, the equations of motion have been linearized and the concept of derivatives is introduced in which the derivatives due to height are included. (The sets of derivatives for various heights, used in the following investigation, are summarized in Table A1. Additional parameters of the chosen configuration are listed in Table A2. See Appendix for both.)

Linearization of the equations of motion leads to a characteristic equation of fifth order,

$$As^5 + Bs^4 + Cs^3 + Ds^2 + Es + F = 0 \tag{9}$$

The coefficients A–F are given in Appendix B as functions of the derivatives and the additional parameters. Equation (9) turns into the well-known fourth-order form for out-of-ground conditions. Then, coefficient F becomes zero because C_{Lz} and C_{mz} equal zero.

In ground effect, three root-locus branches can be derived from Eq. (9). Figure 5 shows the root loci for a height range of $z = H/\bar{c} = 10$ down to 0.5, where $z = 10$ practically represents out-of-ground conditions. The "alpha branch" moves away from the short-period roots and is influenced only slightly by the ground effect. The "P branch" emanates from the low-frequency, low-damping phugoid roots and shows considerable changes in ground effect. This mode becomes unstable at heights below $z = 6$. An aperiodic solution

describes the transients following speed disturbances. In general, this mode is stable.

To simulate flare maneuvers, the chosen aircraft configuration has been equipped with a flight controller. The controller is a simple two-term feedback system using the elevator for controlling the flare, where an ideal flight path, given by

$$\dot{H} = -(1/t_F)H \tag{10}$$

with $t_F = 5$ s, is assumed. The feedback controller commands pitching angular accelerations proportional to the deviations from the ideal flight path in height and in vertical speed, so that

$$\ddot{\vartheta}_R = -V_R(\Delta H + T_v \Delta \dot{H}) \tag{11}$$

In addition, it has been assumed that, by implementing an ideal autothrottle system, the flare is carried out at constant speed.

If the autothrottle system and the two-term controller are introduced, the characteristic equation of the longitudinal motion will be of fourth order with the coefficients summarized in Table B2.

The root-locus plot as a function of the controller gain V_R is shown in Figs. 6 and 7 for heights of $z = 10$ and 1, respectively. The gain varies between $V_R = 0$ and 0.08 rad/s^2·m, while the time constant T_v is kept constant at 2 s. Alpha and P modes behave differently in and out of ground effect. For $z = 10$, the frequency of the P mode is considerably augmented at an increased gain, while the damping ratio is only slightly augmented. The mode becomes unstable for higher gain. The damping ratio of the alpha mode is continuously augmented by increasing the gain. The aperiodic roots are obtained at about $V_R = 0.035$ rad/s^2·m. For $z = 1$, the unstable P mode is induced in stability by increasing the gain and the damping is augmented, but the frequency is kept low. While the P mode remains stable, the alpha mode is destabilized by raising the gain.

It is to be expected that the influence of the ground effect on longitudinal stability must also be noticed in landing, particularly during flareouts. In investigating this relationship, flare maneuvers have been simulated for the chosen aircraft configuration.

Figure 8 shows the ideal flare, corresponding to Eq. (9), compared with a controlled path, without ground effect, for controller gains of $T_v = 2$ s and $V_R = 0.03$ rad/s^2·m. At touchdown, which is assumed to happen at a height of the wing of 3 m, the position and sinking speed are near the ideal values. In Fig. 9, the influence of ground effect is shown. Observe that a considerable deviation from the desired path occurs. In this case, the aircraft will touch the ground much earlier and at a remarkable higher sinking speed. This result can be understood from the root loci (Fig. 7), which show a low-frequency P mode. An increase in the controller gain, unfavorable in any case, will not give much better results. Even when the gain is increased from $V_R = 0.03$ to 0.08 rad/s^2·m, the deviations from the ideal path is not satisfactory (Fig. 10). The observed larger excitation of an oscillating flight path stems from the fact that the higher gain will lead to an unstability of the P mode at greater height (see Fig. 5). Appropriate control laws for the flareout of an aircraft, which is not stable in the P mode at ground proximity, should be investigated in the future.

Summary

Aircraft move close to the ground during takeoff and landing. The influence of the ground on the stability and control characteristics has often been neglected. In this paper, the interrelation between height-dependent aerodynamic coefficients and longitudinal stability is explained and shows particular importance in flare maneuvers. The flight controller for automatic landings should be optimized by considering the basic longitudinal stability characteristics in ground effect.

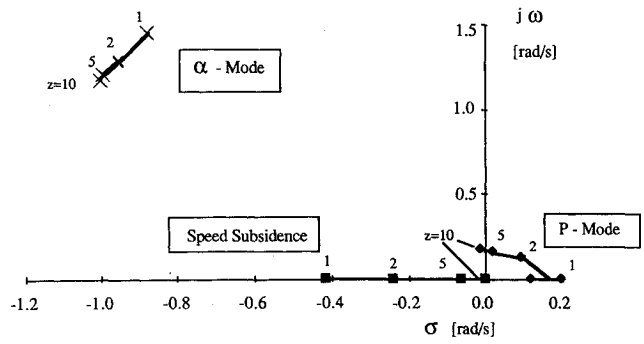

Fig. 5 Root-locus branches depending on height ($z = H/\bar{c}$).

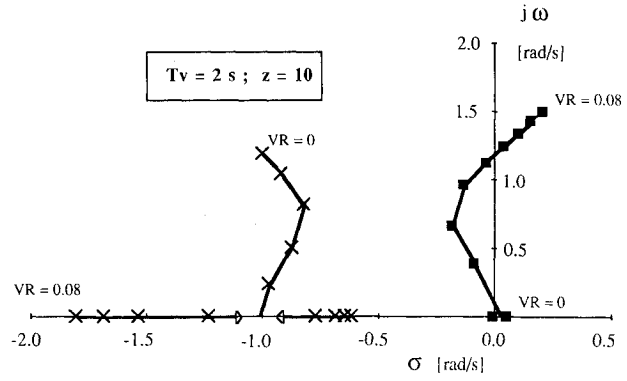

Fig. 6 Root loci for an aircraft with flare controller ($z = 10$).

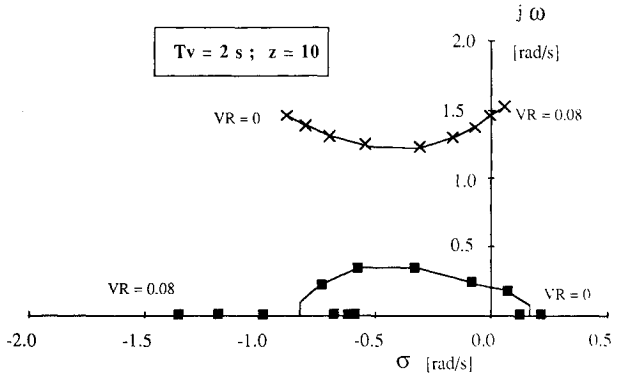

Fig. 7 Root loci for an aircraft with flare controller ($z = 1$).

Appendix A

The equations of longitudinal motion, derivatives of the aerodynamic coefficients, and parameters used in stability investigations and simulations follow.

The longitudinal equations of motion are written in nondimensional form. Wind axes have been used as the reference axes. The three equations can be written as

$$\frac{d\hat{v}}{d\tau} = \frac{T}{W} - C_D\hat{v}^2 - \sin\gamma \tag{A1}$$

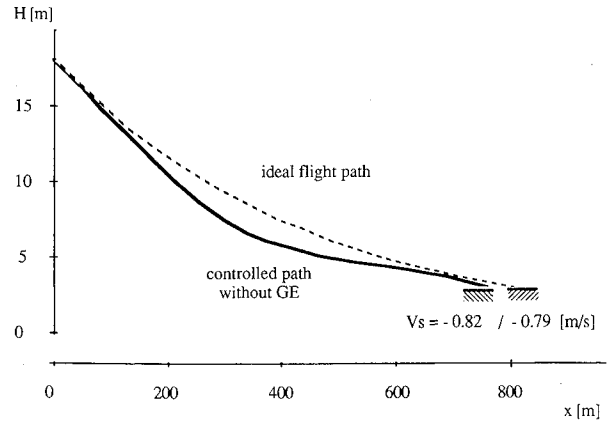

Fig. 8 Flare maneuver without ground effect.

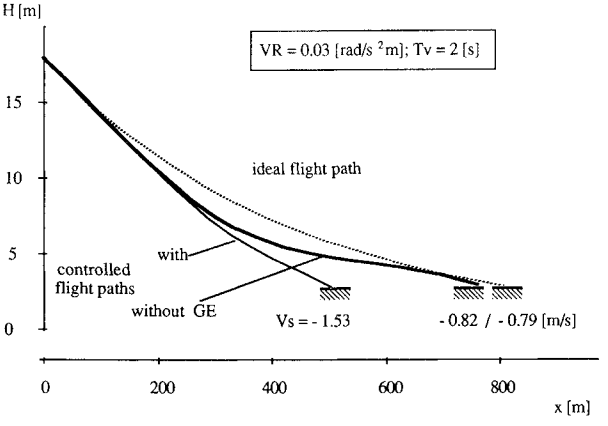

Fig. 9 Flare maneuver with ground effect.

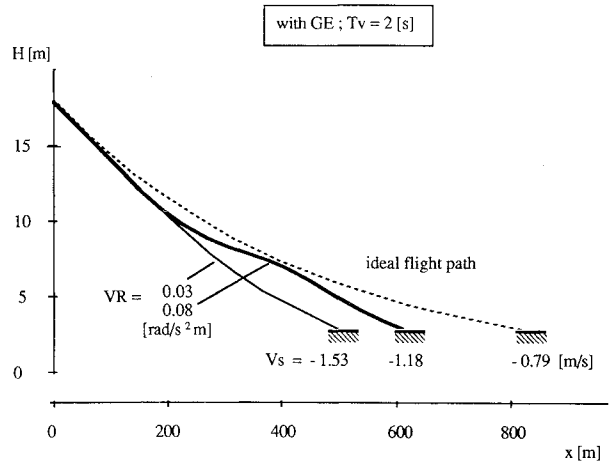

Fig. 10 Flare maneuver with ground effect at various control gains.

$$\hat{v}\frac{d\gamma}{d\tau} = C_L\hat{v}^2 - \cos\gamma \tag{A2}$$

$$\frac{d^2\vartheta}{d\tau^2} = \mu i_y^2 C_m \hat{v}^2 \tag{A3}$$

The kinematic relation is

$$\frac{dz}{d\tau} = \mu\hat{v}\sin\gamma \tag{A4}$$

In general, the aerodynamic coefficients depend on $z = H/\bar{c}$ and α. Equations (A1-A4) have to be solved with given initial conditions and control inputs. For stability investigations, the equations of motion must be linearized. The derivations of the aerodynamic coefficients are written in the form

$$\delta C_D = C_{D\alpha}\delta\alpha + C_{Dz}\delta z \tag{A5a}$$

$$\delta C_L = C_{L\alpha}\delta\alpha + C_{Lz}\delta z \tag{A5b}$$

$$\delta C_m = C_{m\alpha}\delta\alpha + C_{mz}\delta z + \left(\frac{1}{\mu\hat{v}_0}\right)\left[C_{m\dot{\alpha}}\frac{d\alpha}{d\tau} + C_{mq}\frac{d\vartheta}{d\tau}\right] \tag{A5c}$$

Derivatives, used for stability investigations, are given in Table A1 for various heights. The values are valid for an equilibrium state of $C_{L0} = 1.8$ and a static stability margin of $h_n - h = 0.3$ out of ground effect. In addition, parameters of the chosen aircraft configuration are listed in Table A2.

Table A1 Aerodynamic derivatives for $C_{L0} = 1.8$ used in stability investigations and simulations

	$H/\bar{c}$				
Derivative	10	5	2	1	0.5
$C_{L\alpha}$	5.79	5.77	5.52	5.05	4.29
C_{Lz}	0.001	0.003	0.020	0.070	0.034
$C_{D\alpha}$	0.64	0.62	0.44	0.25	0.10
C_{Dz}	0.001	0.004	0.025	0.047	0.061
$C_{m\alpha}$	−1.71	−1.72	−1.93	−2.22	−2.53
C_{mz}	0.001	0.002	0.015	0.041	0.082
$C_{m\dot{\alpha}}$	−4.33	−4.30	−3.69	−2.66	−1.64
C_{mq}	−14.4	−14.4	−14.4	−14.4	−14.4
HS	0.00	0.01	0.06	0.16	0.17

Table A2 Aircraft parameters used in stability investigations and simulations

Wing loading W/S	500 da N/m^2
Wing planform	Rectangular
Aspect ratio	10
$\bar{c}$	5 m
Tail volume	1
$\bar{c}/iy$	1
μ	163
C_{L0}	1.8
$\hat{v}_0$	0.745

Appendix B: Characteristic Equations

Linearizating Eqs. (A1-A4) and substituting Eq. (5) into the equations gives a characteristic equation of the fifth order,

$$As^5 + Bs^4 + Cs^3 + Ds^2 + Es + F = 0 \tag{B1}$$

The coefficients A-F, expressed in terms of derivatives and aircraft parameters, are listed in Table B1. For assisting the landing, a simple control system with an ideal speed control of

$$\hat{v} = \hat{v}_0 = \text{const} \tag{B2}$$

and a two-term controller of

$$\ddot{v}_c = -V_R(\Delta H + T_v\Delta\dot{H}) \tag{B3}$$

is used. Substituting Eqs. (B2) and (B3) into the linearized equations of motion leads to a characteristic equation of the

Table B1 Coefficients of Eq. (B1)

A	1
B	$\hat{v}_0[C_{L\alpha}+2C_{D0}-(C_{m\dot{\alpha}}+C_{mq})l_y^2]$
C	$\hat{v}_0^2[-\mu[C_{Lz}+C_{m\alpha}l_y^2]-C_{L\alpha}C_{m\dot{\alpha}}l_y^2-2C_{D0}(C_{m\dot{\alpha}}+C_{m\dot{q}})l_y^2+2C_{L0}^2+2(C_{D0}C_{L\alpha}-C_{L0}C_{D\alpha})]$
D	$\hat{v}_0^3\{(-2C_{L0}^2+\mu C_{Lz})(C_{m\dot{\alpha}+C_{m\dot{q}}})l_y^2-2C_{D0}[C_{L\alpha}C_{m\dot{\alpha}}l_y^2+\mu(C_{Lz}+C_{m\alpha}l_y^2)]+2C_{L0}[\mu C_{Dz}+C_{D\alpha}C_{m\dot{\alpha}}l_y^2]\}$
E	$\hat{v}_0^4[\mu^2 l_y^2[C_{Lz}C_{m\alpha}-C_{L\alpha}C_{mz}]+2C_{Lz}\mu C_{D0}(C_{m\dot{\alpha}}+C_{m\dot{q}})l_y^2-2C_{L0}[\mu C_{Dz}(C_{m\dot{\alpha}}+C_{m\dot{q}})l_y^2+\mu C_{L0}C_{m\alpha}l_y^2]+2C_{D0}\mu C_{Lz}C_{m\dot{\alpha}}\sigma_\zeta^2]$
F	$\hat{v}_0^5\cdot 2C_{D0}l_y^2\mu^2[(C_{Lz}C_{m\alpha}-C_{L\alpha}C_{mz})+(C_{L0}/C_{D0})(C_{mz}C_{D\alpha}-C_{m\alpha}C_{Dz})]$

Table B2 Coefficients of Eq. (B4) (flight controller included)

A_R	1
B_R	$\hat{v}_0[C_{L\alpha}-l_y^2(C_{m\dot{\alpha}}+C_{mq})]$
C_R	$\hat{v}_0^2[-\mu C_{Lz}-\mu l_y^2 C_{m\alpha}C_{mq}]$
D_R	$\hat{v}_0^3\mu l_y^2[C_{Lz}(C_{m\dot{\alpha}}+C_{mq})+\hat{v}_0 C_{L\alpha}\hat{K}\tau_v]$
E_R	$\hat{v}_0^4\mu l_y^2[\mu(C_{Lz}C_{m\alpha}-C_{L\alpha}C_{mz})+C_{L\alpha}\hat{K}]$

fourth order,

$$A_R s^4+B_R s^3+C_R s^2+D_R s+E_R=0 \tag{B4}$$

the coefficients of which are given in Table B2. The nondimensional control gain $\hat{K}$ is related to V_R by

$$\hat{K}=V_R\frac{\mu\hat{c}^2}{g\hat{v}_0^2 l_y^2} \tag{B5}$$

References

[1]Wieselsberger, C., "Über den Flügelwiderstand in der Nähe des Bodens," *Zeitschift für Flugtechnishe Motorluftschiffahrt,* Vol. 12, 1921, pp. 145–147.

[2]Gratzer, L. B. and Mahal, A. S., "Ground Effects in STOL Operation," *Journal of Aircraft*, Vol. 9, March 1972, pp. 236–242.

[3]Luers, J. K., "Effect of Shear on Aircraft Landing," NASA CR-2287, July 1973.

[4]Kumar, P. E., "An Experimental Investigation into the Aerodynamic Characteristics of a Wing, with and without Endplates in Ground Effect," College of Aerodynamics, Cranfield, England, Rept. Aero 201, 1968.

[5]Staufenbiel, R. and Yeh, B. T. "Flugeigenschaften in der Längsbewegung von Bodeneffekt-Fluggeräten, Teil I and II," ZFW, Vol. 24, 1976, Jan./Feb., pp. 3–9, and March/April, pp. 65–70.

[6]Kleineidam, G., "Ein Beitrag zur Untersuchung der Aerodynamischen und Flugmechanischen Eigenschaften von Profilen in Bodennähe," Dissertation, RWTH, Aachen, FRG, 1981.

[7]Staufenbiel, R. and Kleineidam, G., "Longitudinal Motion of Low-Flying Vehicles in Nonlinear Flowfields," *Proceedings of 12th Congress of the International Council of the Aeronautical Sciences*, Munich, FRG, 1980, pp. 293–308.

[8]Staufenbiel, R., "Some Nonlinear Effect in Stability and Control of Wing-in-Ground Effect Vehicles," *Journal of Aircraft*, Vol. 15, Aug. 1978, pp. 541–544.

[9]Schlichting, U.-J., "Experimentelle und Theoretische Untersuchungen an Tragflügeln und Konfigurationen in Bodennähe," Dissertation, RWTH, Aachen, FRG, 1985.

[10]Barnes, A. G., "Simulating the Visual Approach and Landing," AGARD CP-249, Oct. 1978, pp. 2.1–2.13.

[11]Lippisch, A. M., "Der 'Aerodynamische Bodeneffekt' und die Entwicklung des Flugflächen-(Aerofoil-)Bootes," *Luftfahrttechnik Raumfahrttechnik,* Vol. 10, 1964, pp. 261–269.